EPJ manuscript No.
(will be inserted by the editor)

Chiral Invariant Phase Space Event Generator

II. Nuclear pion capture at rest and photonuclear reactions below the $\Delta(3,3)$ resonance.

P.V. Degtyarenko[1], M.V. Kossov[2], and H.-P. Wellisch[3]

[1] Thomas Jefferson National Accelerator Facility, Newport News, Virginia, USA

[2] Institute of Theoretical and Experimental Physics, Moscow, Russia

[3] CERN, 1211 Geneva, Switzerland

Received: date / Revised version: date

Abstract. An event generator based on the CHIPS model is implemented in the GEANT4 simulation software package. Nuclear fragment production in the process of pion capture on nuclei is used to tune the parameters of the CHIPS model describing clusterization of nucleons in nuclei. The spectra of nucleons and nuclear fragments in pion capture and photonuclear reactions at 60 MeV are compared with experimental data.

PACS. 02.70.Lq Monte Carlo and statistical methods – 12.38.Mh Quark gluon plasma – 21.60.Ka Monte Carlo models in Nuclear structure – 24.10.Lx Monte Carlo simulations (including hadron and parton cascades and string breaking models) in Nuclear reactions: general – 24.85.+p Quarks, gluons, and QCD in nuclei and nuclear processes

1 Introduction

The present publication is the second in a series started with [1], describing the CHIPS model of hadronic fragmentation which we propose to use in the GEANT4 simulation of hadronic processes in the intermediate energy range of nuclear excitations from about 10 MeV to approximately 10 GeV. The main subject of this publication is to consider hadronic fragmentation processes in nuclear matter, where quark exchange reactions are possible between the Quasmon (a droplet of asymptotically free quark-partons, see Ref. [1]) and neighboring nucleons or nuclear clusters.

The CHIPS computer code is a quark-level three-dimensional event generator for the fragmentation of hadronic systems into hadrons. An important feature of the model is a homogeneous distribution of asymptotically free

quark-partons over the invariant phase space, applied to the fragmentation of different types of excited hadronic systems including nucleon excitations, hadronic systems produced in e^+e^- interactions, high energy nuclear excitations, etc. Exclusive event generation which models multiple hadron production conserving energy, momentum, and charge generally results in a good description of particle multiplicities and spectra in multihadron fragmentation processes. All this makes it possible to use the event generator in exclusive modeling of hadron cascades in materials.

As compared with the first "in vacuum" version of the model, described in [1], modeling of hadronic fragmentation in nuclear matter is more complicated because of the much greater number of possible secondary fragments, but the hadronization process itself is simpler in a certain way. In vacuum, the quark-fusion mechanism requires a quark-parton partner from the external (as in JETSET [2]) or internal (Quasmon itself [1]) quark-antiquark sea. In nuclear matter, there is another possibility of quark exchange with the neighboring hadronic system, nucleon or nuclear multinucleon cluster. Thus in nuclear matter the spectra of secondary hadrons and nuclear fragments may be considered as a reflection of the quark-parton spectrum in a Quasmon. In the case of inclusive spectra that are steeply decreasing with energy, and correspondingly steeply decreasing spectra of the quark-partons in a Quasmon, only those secondary hadrons which get the maximum energy from the primary quark-parton with energy k are contributing to the inclusive spectra. This extreme situation requires the exchanged quark-parton with energy q, coming back to the Quasmon from the cluster, to move in the opposite direction with respect to the primary quark-parton. As a result the hadronization quark exchange process becomes one-dimensional along the direction of k. If a neighboring nucleon or nuclear cluster with bound mass $\tilde{\mu}$ absorbs the primary quark-parton and radiates the exchanged quark-parton in the opposite direction, then the energy of the outgoing fragment is $E = \tilde{\mu} + k - q$, and the momentum is $p = k + q$. Both energy and momentum of the outgoing nuclear fragment are known (as well as the mass $\tilde{\mu}$ of the nuclear fragment in nuclear matter), so the momentum of the primary quark-parton can be reconstructed using the approximate relation

$$k = \frac{p + E - B \cdot m_N}{2}, \qquad (1)$$

where B is the baryon number of the outgoing fragment ($\tilde{\mu} \approx B \cdot m_N$, where m_N is the nucleon mass). In [3] it was shown that the invariant inclusive spectra of pions, protons, deuterons, and tritons in proton-nucleus reactions at 400 GeV [4] have not only the same exponential slope but almost coincide when they are plotted as a function of $k = \frac{p+E_{\rm kin}}{2}$. Using data at 10 GeV [5], it was shown that the parameter k defined by equation (1) is appropriate also for the description of secondary antiprotons produced in high energy nuclear reactions. This means that the extreme assumption of one-dimensional hadronization is a good approximation, not only for the quark exchange mechanism but for the quark fusion mechanism, too. In the one-dimensional case, assuming that q is the momentum of the second quark fusing with the primary quark-

parton with energy k, the total energy of the outgoing hadron is $E = q + k$ and the momentum $p = k - q$. In the one-dimensional case the secondary quark-parton must still move in the opposite direction with respect to the primary quark-parton; otherwise the mass of the outgoing hadron would be zero. So we get for mesons $k = \frac{p+E}{2}$, in accordance with equation (1). In the case of antiproton radiation the baryon number of the Quasmon is increased by one, and the primary antiquark-parton will spend its energy to build up the mass of the antiproton by picking up an anti-diquark. Thus, the energy conservation law for antiproton radiation looks like $E + m_N = q + k$ and hence $k = \frac{p+E+m_N}{2}$, which is again in accordance with equation (1).

This one-dimensional quark exchange mechanism was proposed in 1984 [3]. Even in its approximate form it was useful in the analysis of inclusive spectra of hadrons and nuclear fragments in hadron-nuclear reactions at high energies. Later the same approach was used in the analysis of nuclear fragmentation in electro-nuclear reactions [6]. Also in 1984 the quark-exchange mechanism developed in the framework of the non-relativistic quark model was found to be important for the explanation of the short distance features of NN interactions [7]. Later it was successfully applied to K^-p interactions [8]. The idea of the quark exchange mechanism between nucleons was useful even for the explanation of the EMC effect [9]. For the non-relativistic quark model the quark exchange technique was developed as an alternative to the Feynman diagram technique at short distances [10].

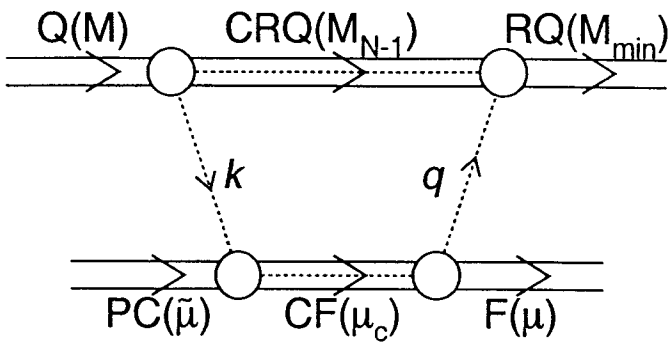

Fig. 1. Diagram of quark exchange mechanism.

The CHIPS event generator models quark exchange processes taking into account kinematical and combinatorial factors for asymptotically free quark-partons. The naive picture of the quark-exchange mechanism is tunneling of quark-partons from the asymptotically free region of one hadron to the asymptotically free region of another hadron. To conserve color, another quark-parton from the neighboring hadron must replace the first quark-parton in the Quasmon. It makes the tunneling mutual, and the process has to be quark exchange.

The experimental data available on multihadron production at high energies show regularities in the secondary particle spectra that can be related to the simple kinematical, combinatorial, and phase space rules of such quark exchange and fusion mechanisms. The CHIPS model combines these mechanisms consistently in the form of a computational algorithm and an event generator.

2 Algorithm of quark exchange calculation.

Figure 1 shows the quark exchange diagram which helps to keep track of the kinematics of the quark-exchange process. It was shown in Ref. [1] that a Quasmon (Q in Fig. 1)

is kinematically determined by a few asymptotically free quark-partons homogeneously distributed over the invariant phase space. The Quasmon mass M is related to the number of quark-partons N:

$$< M^2 >= 4N(N-1)\cdot T^2, \tag{2}$$

where T is the temperature of the system.

The spectrum of quark partons can be calculated as

$$\frac{dW}{k^* dk^*} \propto \left(1 - \frac{2k^*}{M}\right)^{N-3}, \tag{3}$$

where k^* is the energy of the primary quark-parton in the center-of-mass system (CMS) of the Quasmon. After the primary quark-parton is randomized and the neighboring cluster (parent cluster – PC in Fig. 1) with the bound mass $\tilde{\mu}$ is selected, the quark exchange process starts. To follow the process kinematically one should imagine a colored compound system consisting of the bound parent cluster and the primary quark with energy k in the laboratory system (LS)

$$k = k^* \cdot \frac{E_N + p_N \cdot \cos(\theta_k)}{M_N}, \tag{4}$$

where M_N, E_N and p_N are mass, energy, and momentum of the Quasmon in the LS. The mass of the compound system (CF in Fig. 1) is $\mu_c = \sqrt{(\tilde{\mu}+k)^2}$, where $\tilde{\mu}$ and k are four-vectors. This colored compound system should decay into a free outgoing nuclear fragment with mass μ (F in Fig. 1) and the recoiling quark with energy q (in CMS of $\tilde{\mu}$, which coincides with LC in the present version of the model as no internal motion of clusters is considered). At this point one should recall that the colored residual Quasmon with mass M_{N-1} (CRQ in Fig. 1) is left after radiation of k. The last act is to fuse the CRQ and the recoil quark q. The resulting residual quasmon (RQ in Fig. 1) should have its minimum mass higher than $M_{\min}$, which is determined by the minimum mass of a hadron (or Chipolino, double-hadron as defined in Ref. [1]) with the same quark content. All quark-antiquark pairs with the same flavor should be canceled in the minimum mass calculations. In CMS of μ_c this restriction can be written as

$$2q \cdot (E - p \cdot \cos\theta_{qCQ}) + M_{N-1}^2 > M_{\min}^2 \tag{5}$$

where E is the energy and p is the momentum of the colored residual Quasmon with mass M_{N-1} in CMS of μ_c. Then the restriction for $\cos\theta_{qCQ}$ is

$$\cos\theta_{qCQ} < \frac{2qE - M_{\min}^2 + M_{N-1}^2}{2qp}. \tag{6}$$

This means that

$$q > \frac{M_{N-1}^2 - M_{\min}^2}{2\cdot(E+p)}. \tag{7}$$

Another restriction comes from the nuclear Coulomb barrier for charged particles. We calculate the Coulomb barrier in a simple form:

$$E_{CB} = \frac{Z_F \cdot Z_R}{A_F^{\frac{1}{3}} + A_R^{\frac{1}{3}}}\ (\text{MeV}), \tag{8}$$

where Z_F and A_F are charge and atomic weight of the fragment, and Z_R and A_R are charge and atomic weight of the residual nucleus. The obvious restriction is

$$q < k + \tilde{\mu} - \mu - E_{CB}. \tag{9}$$

The restrictions (7) and (9) are complementary to the restrictions from the quark exchange mechanism which

should be calculated. The spectrum of recoiling quarks is similar to the k^* spectrum in Quasmon (3):

$$\frac{dW}{q\,dq\,d\cos\theta} \propto \left(1-\frac{2q}{\tilde{\mu}}\right)^{n-3}, \qquad (10)$$

where n is a number of quark-partons in the nuclear cluster. We consider it to be equal to $3A_C$, where A_C is the atomic weight of the parent cluster. Tunneling of quarks from one nucleon to another makes the phase space common for all quark-partons of the cluster.

An additional equation follows from the mass shell condition for the outgoing fragment:

$$\mu^2 = \tilde{\mu}^2 + 2\tilde{\mu}\cdot k - 2\tilde{\mu}\cdot q - 2k\cdot q\cdot(1-\cos\theta_{kq}), \qquad (11)$$

where θ_{kq} is the angle between quark-partons in LS. From this equation q can be calculated as

$$q = \frac{\tilde{\mu}\cdot(k-\Delta)}{\tilde{\mu}+k\cdot(1-\cos\theta_{kq})}, \qquad (12)$$

where Δ is the covariant binding energy of the cluster $\Delta = \frac{\mu^2-\tilde{\mu}^2}{2\tilde{\mu}}$. The quark exchange probability integral can be written in the form:

$$P(k,\tilde{\mu},\mu) = \int \delta\left[\mu^2-\tilde{\mu}^2-2\tilde{\mu}\cdot k+2\tilde{\mu}\cdot q+2k\cdot q\cdot(1-\cos\theta_{kq})\right] \times \left(1-\frac{2q}{\tilde{\mu}}\right)^{n-3} qdq\cdot d\cos\theta_{kq}. \qquad (13)$$

Using the δ-function to make the integration over q one can get:

$$P(k,\tilde{\mu},\mu) = \int \left(1-\frac{2(k-\Delta)}{\tilde{\mu}+k(1-\cos\theta_{kq})}\right)^{n-3} \times \frac{\tilde{\mu}(k-\Delta)}{2[\tilde{\mu}+k(1-\cos\theta_{kq})]^2} d\cos\theta_{kq} \qquad (14)$$

or

$$P(k,\tilde{\mu},\mu) = \int \left(1-\frac{2(k-\Delta)}{\tilde{\mu}+k(1-\cos\theta_{kq})}\right)^{n-3} \times \left(\frac{\tilde{\mu}(k-\Delta)}{\tilde{\mu}+k(1-\cos\theta_{kq})}\right)^2 \times d\left(\frac{\tilde{\mu}+k(1-\cos\theta_{kq})}{\tilde{\mu}(k-\Delta)}\right). \qquad (15)$$

The result of the integration is

$$P(k,\tilde{\mu},\mu) = \frac{\tilde{\mu}}{4k(n-2)} \times \left[\left(1-\frac{2(k-\Delta)}{\tilde{\mu}+2k}\right)^{n-2}_{\text{high}} - \left(1-\frac{2(k-\Delta)}{\tilde{\mu}}\right)^{n-2}_{\text{low}}\right] \qquad (16)$$

For randomization it is convenient to make z a random parameter

$$z = 1-\frac{2(k-\Delta)}{\tilde{\mu}+k(1-\cos\theta_{kq})} = 1-\frac{2q}{\tilde{\mu}}. \qquad (17)$$

From (16) one can find the high and the low limits of the randomization. The first limit is a limit for k: $k > \Delta$. It is similar to the restriction for Quasmon fragmentation in vacuum: $k^* > \frac{\mu^2}{2M}$. The second limit is $k = \frac{\mu^2}{2\tilde{\mu}}$, when the low limit of randomization becomes equal to zero. If $k < \frac{\mu^2}{2\tilde{\mu}}$, then $-1 < \cos\theta_{kq} < 1$ and $z_{\text{low}} = 1-\frac{2(k-\Delta)}{\tilde{\mu}}$. If $k > \frac{\mu^2}{2\tilde{\mu}}$, then the range of $\cos\theta_{kq}$ is $-1 < \cos\theta_{kq} < \frac{\mu^2}{k\tilde{\mu}}-1$ and $z_{\text{low}} = 0$. This value of z_{low} should be corrected using the Coulomb barrier restriction (9), and the value of z_{high} should be corrected using the minimum residual Quasmon restriction (7). In the case of a Quasmon with momentum much less than k it is possible to impose a tighter restriction than (7) because the direction of motion of the CRQ is opposite to k. So $\cos\theta_{qCQ} = -\cos\theta_{kq}$, and from (12) one can find that

$$\cos\theta_{qCQ} = 1-\frac{\tilde{\mu}\cdot(k-\Delta-q)}{k\cdot q}. \qquad (18)$$

So in this case the equation (7) transforms into a more stringent one:

$$q > \frac{M^2_{N-1}-M^2_{\text{min}}+2\frac{p\cdot\tilde{\mu}}{k}(k-\Delta)}{2\cdot(E+p+\frac{p\cdot\tilde{\mu}}{k})}. \qquad (19)$$

The integrated kinematical quark exchange probability (in the range from $z_{\rm low}$ to $z_{\rm high}$) is

$$\frac{\tilde{\mu}}{4k(n-2)} \cdot z^{n-2} \tag{20}$$

and the total kinematical probability of hadronization of the quark-parton with energy k into a nuclear fragment with mass μ is

$$\frac{\tilde{\mu}}{4k(n-2)} \cdot \left(z_{\rm high}^{n-2} - z_{\rm low}^{n-2}\right). \tag{21}$$

This can be compared with the vacuum probability of the quark fusion mechanism [1]:

$$\frac{M-2k}{4k(N-3)} z_{\rm max}^{N-3}. \tag{22}$$

The similarity is very important as the absolute probabilities define the competition between vacuum and nuclear channels.

Equations (20) and (21) can be used for randomization of z:

$$z = z_{\rm low} + \sqrt[n-2]{R} \cdot (z_{\rm high} - z_{\rm low}), \tag{23}$$

where R is a random number uniformly distributed in the interval (0,1).

Equation (21) can be used to control the competition between different nuclear fragments and hadrons in the hadronization process. In the comparison with the vacuum hadronization it is not enough to take only into account the quark combinatorics of the Quasmon and the outgoing hadron. In case of hadronization in nuclear matter, different parent bound clusters should be taken into account, too. For example, tritium can be radiated as a result of quark exchange with a bound tritium cluster or as a result of quark exchange with a bound ^{3}He cluster.

To calculate the yield of fragments it is necessary to calculate the probability to find a cluster with certain proton and neutron content in a nucleus. In fact one can consider any particular probability as an independent parameter. In such a case the process of tuning the model would be difficult. We proposed the following scenario of clusterization. A gas of quasi-free nucleons is close to the phase transition into the liquid phase bound by strong quark exchange forces. Precursors of the liquid phase are nuclear clusters, which may be considered as "drops" of the liquid phase in the nucleus. Any cluster can meet another nucleon and absorb it (making it bigger), or it can release one of the nucleons (making it smaller). The first parameter ε_1 is the percentage of quasi-free nucleons not involved in the clusterization process. The rest of the nucleons $(1-\varepsilon_1)$ clusterize differently. We assume that on the periphery of the nucleus the density is lower, and one can consider only dibaryon clusters, as the number of triple-baryon clusters is negligible there. Still we denote the number of nucleons clusterized in dibaryons on the periphery by the parameter ε_2. In the dense part of the nucleus, strong quark exchange forces make clusters out of quasi-free nucleons with high probability. To calculate the distribution of clusters the parameter ω of clusterization probability was used.

If the number of nucleons involved in clusterization is $a = (1-\varepsilon_1-\varepsilon_2) \cdot A$, then the probability to find a cluster consisting of ν nucleons is

$$P_\nu \propto C_\nu^a \cdot \omega^{\nu-1}. \tag{24}$$

The coefficient of proportionality can be found from the equation

$$a = b \cdot \sum_{\nu=1}^{a} \nu \cdot C_\nu^a \cdot \omega^{\nu-1} = b \cdot a \cdot (1+\omega)^{a-1}. \qquad (25)$$

Thus, the number of clusters consisting of ν nucleons is

$$P_\nu = \frac{C_\nu^a \cdot \omega^{\nu-1}}{(1+\omega)^{a-1}}. \qquad (26)$$

For clusters with an even number of nucleons we used only isotopically symmetric configurations ($\nu = 2n$, n protons and n neutrons) and for odd clusters ($\nu = 2n+1$) we used only two configurations: n neutrons with $n+1$ protons and $n+1$ neutrons with n protons. This restriction, which we call "isotopic focusing", can be considered as an empirical rule of the CHIPS model which helps to describe data. It is applied in the case of nuclear clusterization (isotopically symmetric clusters) and in the case of hadronization processes in nuclear matter. In hadronization processes the Quasmon is shifted from isotopic symmetric state (e.g., by capturing a negative pion) and transfers excessive charge to the outgoing nuclear cluster. This tendency is symmetric with respect to the Quasmon and the parent cluster.

The temperature parameter used to calculate the number of quark-partons in the Quasmon (see equation 2) was chosen to be $T = 180$ MeV, same as in Ref. [1].

The CHIPS model is mostly a model of chaotic fragmentation conserving energy, momentum, and charge. But to compare it with experimental data one needs to model also the first interaction of the projectile with the nucleus. For proton-antiproton annihilation this was easy, as we assumed that in the interaction at rest, a proton and antiproton always create a Quasmon. In the case of pion capture the pion can be captured by different clusters. We assumed that the probability of capture is proportional to the number of nucleons in a cluster. After the capture the Quasmon is formed, and the CHIPS generator then produces fragments consecutively and recursively, choosing at each step the quark-parton four-momentum k, type of parent and outgoing fragment, and the four-momentum of the exchange quark-parton q, to produce a final state hadron and the new Quasmon with less energy.

In the CHIPS model we consider the whole process as a chaotic process with large number of degrees of freedom and do not take into account any final state interactions of outgoing hadrons. Nevertheless, when the excitation energy dissipates, and on some step the Quasmon mass drops below mass shell, the quark-parton mechanism of hadronization fails. To model the event exclusively, it becomes necessary to continue fragmentation at the hadron level. Such fragmentation process is known as nuclear evaporation. It is modeled using the non-relativistic phase space approach. In the non-relativistic case the phase space of nucleons can be integrated as well as in the ultra-relativistic case of quark-partons.

The general formula for the non-relativistic phase space can be found starting with the phase space for two particles $\tilde{\Phi}_2$. It is proportional to the CMS momentum:

$$\tilde{\Phi}_2(W_2) \propto \sqrt{W_2}, \qquad (27)$$

where W_2 is a total kinetic energy of the two non-relativistic particles. If the phase space integral is known for $n-1$ hadrons then it is possible to calculate the phase space

integral for n hadrons:

$$\tilde{\Phi}_n(W_n) = \int \tilde{\Phi}_{n-1}(W_{n-1}) \cdot \delta(W_n - W_{n-1} - E_{\rm kin}) \times \sqrt{E_{\rm kin}} dE_{\rm kin} dW_{n-1}. \quad (28)$$

Using (27) and (28) one can find that

$$\tilde{\Phi}_n(W_n) \propto W_n^{\frac{3}{2}n-\frac{5}{2}} \quad (29)$$

and the spectrum of hadrons, defined by the phase space of residual $n-1$ nucleons, can be written as

$$\frac{dN}{\sqrt{E_{\rm kin}} dE_{\rm kin}} \propto \left(1 - \frac{E_{\rm kin}}{W_n}\right)^{\frac{3}{2}n-4}. \quad (30)$$

This spectrum can be randomized. The only problem is from which level one should measure the thermal kinetic energy when most nucleons in nuclei are filling nuclear levels with zero temperature. To model the evaporation process we used this unknown level as a parameter U of the evaporation process. Comparison with experimental data gives $U = 1.7$ MeV. Thus, the total kinetic energy of A nucleons is

$$W_A = U \cdot A + E_{\rm ex}, \quad (31)$$

where $E_{\rm ex}$ is the excitation energy of the nucleus.

To be radiated, the nucleon should overcome the threshold

$$U_{\rm thresh} = U + U_{\rm bind} + E_{CB}, \quad (32)$$

where $U_{\rm bind}$ is a separation energy of the nucleon, and E_{CB} is the Coulomb barrier energy which is non-zero only for positive particles and can be calculated using formula (8).

3 Comparison with data

Among several experimental investigations of nuclear pion capture at rest we have selected four published results which constitute, in our opinion, a representative data set covering a wide range of target nuclei, types of produced hadrons and nuclei fragments, and their energy range. In the first publication [11] the spectra of charged fragments (protons, deuterons, tritium, ^{3}He, ^{4}He) in the pion capture reaction were measured on 17 nuclei within one experimental setup. To verify the spectra we compared them for a carbon target with detailed measurements of the spectra of charged fragments given in Ref. [12]. In addition, we took ^{6}Li spectra for a carbon target from the same paper.

The neutron spectra were added from Ref. [13] and Ref. [14]. We present data and Monte Carlo distributions as the invariant phase space function $f = \frac{d\sigma}{pdE}$ depending on the variable $k = \frac{p+E_{\rm kin}}{2}$ as defined in equation (1).

Spectra on ^{9}Be, ^{12}C, ^{28}Si (^{27}Al for secondary neutrons), ^{59}Co (^{64}Cu for secondary neutrons), and ^{181}Ta are shown in Figures 2 through 6. The data are described well, including the total energy spent in the reaction to yield the particular type of fragments.

The evaporation process for nucleons is described well, too. It is exponential in k, and looks especially impressive for Si/Al and Co/Cu data, where the Coulomb barrier is low, and one can see proton evaporation as a continuation of the evaporation spectra from secondary neutrons. This way the exponential behavior of the evaporation process can be followed over 3 orders of magnitude. Clearly seen is the transition region at $k \approx 90$ MeV (kinetic energy

Table 1. Clusterization parameters

	^{9}Be	^{12}C	^{28}Si	^{59}Co	^{181}Ta
ε_1	0.45	0.40	0.35	0.33	0.33
ε_2	0.15	0.15	0.05	0.03	0.02
ω	5.00	5.00	5.00	5.00	5.00

$15-20$ MeV) between the quark-level hadronization process and the hadron-level evaporation process. For light target nuclei the evaporation process becomes much less prominent.

The ^{6}Li spectrum on a carbon target exhibits an interesting regularity when plotted as a function of k: it practically coincides with the spectrum of ^{4}He fragments, and shows exponential behavior in a wide range of k, corresponding to a few orders of magnitude in the invariant cross section. To keep the figure readable, we did not plot the ^{6}Li spectrum generated by CHIPS. It coincides with the ^{4}He spectrum at $k > 200$ MeV, and underestimates lithium emission at lower energies, similarly to the ^{3}He and tritium data.

Between the region where hadron-level processes dominate and the kinematic limit all hadronic spectra slopes become close when plotted as a function of k. In addition to this general behavior there is an effect of strong proton-neutron splitting. For protons and neutrons it reaches almost an order of magnitude. To model such splitting in the CHIPS generator, the mechanism of "isotopic focusing" was used, which locally transfers the negative charge from the pion to the first radiated nuclear fragment.

Thus, the model qualitatively describes all typical features of the pion capture process. The question is what can be extracted from the experimental data with this tool. The clusterization parameters are listed in Table 1. No formal fitting procedure has been performed. A balanced qualitative agreement with all data was used to tune the parameters. The difference between the $\frac{\varepsilon_2}{\varepsilon_1}$ ratio and the parameter ω (which is the same for all nuclei) is an indication that there is a phase transition between the gas phase and the liquid phase of the nucleus. The large value of the parameter ω, determining the average size of the nuclear cluster, is critical in describing the model spectra at large k, where the fragment spectra approach the kinematical limits.

Using the same parameters of clusterization we compared the data [15] on γ absorption on Al and Ca nuclei (Fig. 7) with the CHIPS results. One can see that the spectra of secondary protons and deuterons are qualitatively described by the CHIPS model.

GEANT4 implementation

As compared with the previous "in vacuum" version, the developed version of the CHIPS model is more organized. For nuclear masses it uses the standard GEANT4 tools. For nuclear reactions at low energies where the deposited energy is comparable with the binding energy of nucleons and nuclear clusters the knowledge of the masses of the ground state nuclei becomes very important. In addition, a Q-World of the CHIPS model is created at the first call of the G4Quasmon class. All pointers to the Q-World are

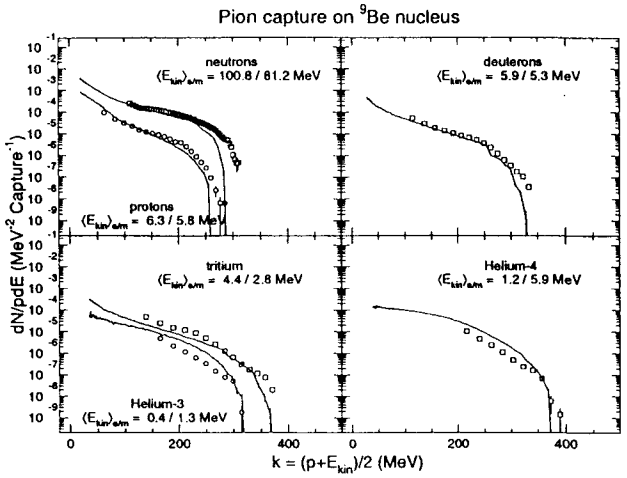

Fig. 2. Comparison of the CHIPS model results with experimental data on proton, neutron, and nuclear fragment production in the capture of negative pions on ^{9}Be. Proton [11] and neutron [13] experimental spectra are shown in the upper left panel by open circles and open squares, respectively. The model calculations are shown by the two corresponding solid lines. The same arrangement is used to present ^{3}He [11] and tritium [11] spectra in the lower left panel. Deuterium [11] and ^{4}He [11] spectra are shown in the right panels of the figure by open squares and lines (CHIPS model). The average kinetic energy carried away by each nuclear fragment is shown in the panels by the two numbers: first is the average calculated using the experimental data shown; second is the model result.

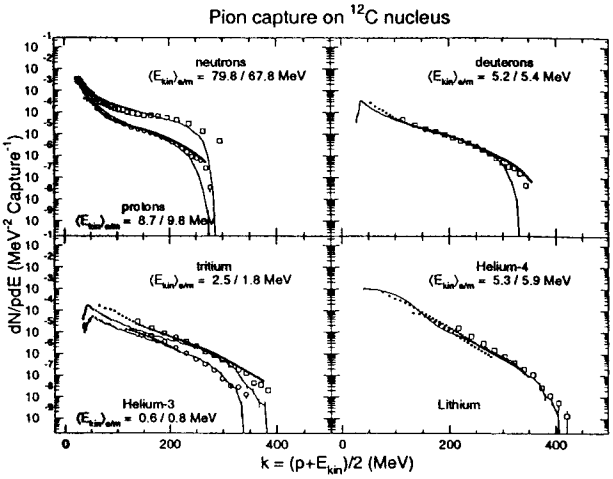

Fig. 3. Same as in Figure 2, for pion capture on ^{12}C. The experimental neutron spectrum is taken from [14]. In addition, the detailed data on charged particle production, including the ^{6}Li spectrum, taken from Ref. [12], are superimposed on the plots as a series of dots.

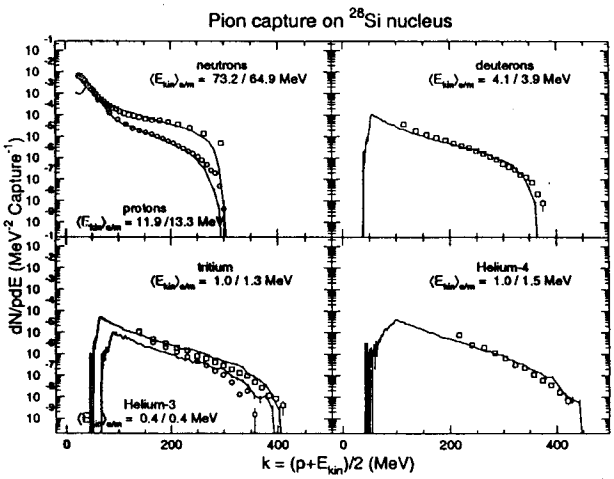

Fig. 4. Same as in Figure 2, for pion capture on ^{28}Si nucleus. The experimental neutron spectrum is taken from [14], for the reaction on ^{27}Al.

kept as static parameters of the class, so any new C++ instance of the class can immediately connect itself to the Q-World resident in memory. A special destructive member function of the G4Quasmon class can destroy the Q-World, cleaning up a space in the C++ heap. This procedure releases memory but requires rebuilding the Q-World when a new C++ instance of the G4Quasmon class is created.

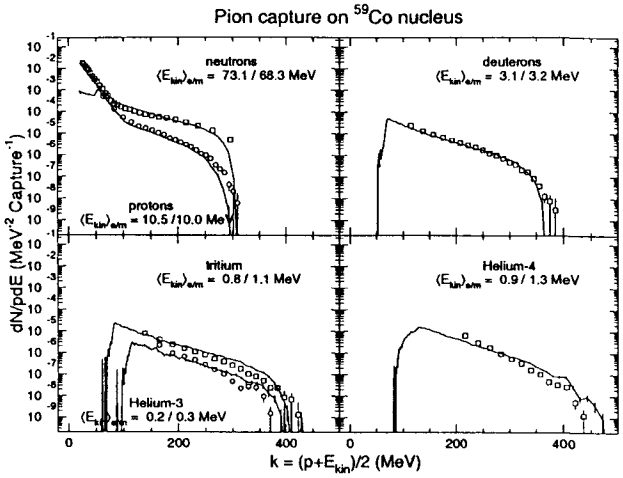

Fig. 5. Same as in Figure 2, for pion capture on ^{59}Co. The experimental neutron spectrum is taken from [14], for the reaction on ^{64}Cu.

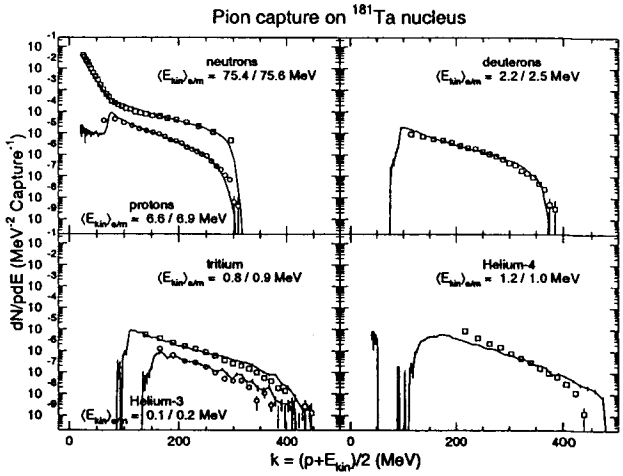

Fig. 6. Same as in Figure 2, for pion capture on ^{181}Ta. The experimental neutron spectrum is taken from [14].

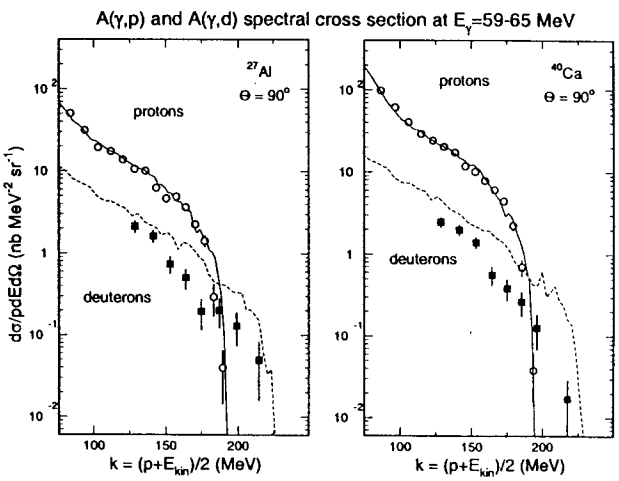

Fig. 7. Comparison of CHIPS model with experimental data [15] on proton and deuteron production at 90° in photonuclear reactions on ^{27}Al and ^{40}Ca at 59 – 65 MeV. Open circles and solid squares represent the experimental proton and deuteron spectra, respectively. Solid and dashed lines show the results of the corresponding CHIPS model calculation. Statistical errors in the CHIPS results are not shown and can be judged by the point-to-point variations in the lines. The comparison is absolute, using the values of total photonuclear cross section 3.6 mb for Al and 5.4 mb for Ca, as given in Ref. [16].

The Q-World includes C++ objects – instances of particles and nuclear fragments. Each particle has a vector of decay channels, and any decay channel includes a branching ratio and a vector of secondary particles. At this time the Q-World includes 71 particles and 53 anti-particles. Nuclear fragments of the Q-World are covering n/p-symmetri nuclei and hypernuclei with strangeness less than 3. For example, for $A = 6$ nuclei there are ^{6}He, ^{6}Li, ^{6}Be, ^{5}He$_{\Lambda}$, ^{5}Li$_{\Lambda}$, ^{4}H$_{\Lambda\Lambda}$, ^{4}He$_{\Lambda\Lambda}$, and ^{4}Li$_{\Lambda\Lambda}$. All particles of the Q-World have a Q-Code and a PDG-Code. The Q-Code numerates the particles and fragments. It works as a sequential ID for particle data bases, and the PDG-code is the code of the Particle Data Group. To implement fragments in the Q-World any fragment has a PDG-code in the form: $9SZZZNNN$. The PDG-code of a nucleus in the Q-World consists of 8 digits. The first digit following the PDG convention is 9; the second digit is the number of Λ particles

in the nucleus. It is restricted to 9 Λ particles in a nucleus or nuclear fragment. Digits from 3 to 5 give the number of protons, and digits from 6 to 8 give the number of neutrons. Three particles (p, n, and Λ) are represented in the Q-World twice: the first time as hadrons created in a vacuum as a result of quark fusion hadronization, and the second time as nuclear fragments created in the nuclear medium as a result of quark exchange hadronization. So for these baryons it is possible to find out from their PDG-codes how they were created.

In addition, at any step of the fragmentation a vector of candidates for the outgoing fragment (hadron or nuclear fragment) is created. If the candidate is a nuclear fragment then it has a vector of possible parent clusters from the nuclear environment. For each candidate a probability of hadronization is calculated, and for nuclear fragments subprobabilities for different parent clusters are calculated, too.

All unstable (with respect to strong interaction) particles, including p-, n-, and α-unstable nuclei, decay in the sequence. The evaporation process is organized as a sequential decay of the excited nucleus. The information about the parent nucleus can be found in the vector of output hadrons. A user is able to decide what to do with it. For example, in the case of relatively long lifetime α-unstable nuclei, like ^{8}Be, in certain circumstances it might be necessary to use explicitly the ^{8}Be parent nucleus in the cascade to model the energy loss in the event correctly.

4 Conclusion

The CHIPS model covers a wide spectrum of hadronic reactions with a large number of degrees of freedom. In the case of nuclear reactions the CHIPS generator helps to understand phenomena such as an order of magnitude splitting of neutron and proton spectra, high yield of energetic nuclear fragments, and emission of nucleons which kinematically can be produced only if seven or more nucleons are involved in the reaction.

The CHIPS generator lets us extract collective parameters of a nucleus such as clusterization. The qualitative conclusion based on the fit to the experimental data is that the main fraction of nucleons is clusterized, at least in heavy nuclei. The nuclear clusters can be considered as drops of a liquid nuclear phase. The quark exchange makes the phase space of quark-partons of the cluster common, stretching kinematic limits for particle production.

The hypothetical quark exchange process is important not only for the nuclear clusterization but for the nuclear hadronization process, too. The quark exchange between the excited cluster (Quasmon) and a neighboring nuclear cluster even at low excitation level operates with quark-partons at energies comparable with the nucleon mass. As a result it easily reaches the kinematic limits of the reaction, revealing the multinucleon nature of the process.

Up to now the most underdeveloped part of the model has been the initial interaction between projectile and target. That is why we started with proton-antiproton annihilation and pion capture on nuclei at rest, which do not involve any interaction cross section. The further devel-

opment of the model will require a better understanding of the mechanism of the first interaction. However, we believe that even the basic model will be useful in understanding the nature of multihadron fragmentation, and because of its features, is a suitable candidate for the hadron production and hadron cascade parts of the newly developed event generation and detector simulation Monte Carlo computer codes.

Acknowledgment

The work was supported by the US Department of Energy under contract number DE-AC05-84ER4015.

References

1. P.V. Degtyarenko, M.V. Kossov, H.-P. Wellisch, to be published.
2. T. Sjöstrand, Comp. Phys. Comm. **92** (1994) 74.
3. M.V. Kossov and L.M. Voronina, Preprint ITEP 165-84, Moscow (1984).
4. V.I. Efremenko et al., Phys. Rev. C **22** (1980) 700.
5. S.V Boyarinov et al., Phys. At. Nucl. **56** (1993) 72.
6. P. V. Degtyarenko et al., Phys. Rev. C **50**(1994) R541.
7. K. Maltman and N. Isgur, Phys. Rev. D **29** (1984) 952.
8. K. Maltman and N. Isgur, Phys. Rev. D **34** (1986) 1372.
9. P. Hoodbhoy and R. J. Jaffe, Phys. Rev. D **35** (1987) 113.
10. N. Isgur, Nucl. Phys. **A497** (1989) 91.
11. A. I. Amelin et al., "Energy spectra of charged particles in the reaction of π^- absorption at rest by ^{6,7}Li, ^{9}Be, ^{10,11}B, ^{12}C, ^{28}Si, ^{40}Ca, ^{59}Co, ^{93}Nb, ^{114,117,120,124}Sn, ^{169}Tm, ^{181}Ta and ^{209}Bi nuclei", Moscow Physics and Engineering Institute Preprint No. 034-90, Moscow, 1990.
12. G. Mechtersheimer et al., Nucl. Phys. **A324** (1979) 379.
13. C. Cernigoi et al., Nucl. Phys. **A456** (1986) 599.
14. R. Madey et al., Phys. Rev. C **25** (1982) 3050.
15. D. Ryckbosch et al., Phys. Rev. C **42** (1990) 444.
16. J. Ahrens et al., Nucl. Phys. **A446** (1985) 229c.